The Timothy syndrome mutation differentially affects voltage- and calcium-dependent inactivation of $Ca_V1.2$ L-type calcium channels

Curtis F. Barrett* and Richard W. Tsien†

Department of Molecular and Cellular Physiology, Stanford University School of Medicine, Stanford, CA 94305-5345

Contributed by Richard W. Tsien, November 7, 2007 (sent for review September 6, 2007)

Calcium entry into excitable cells is an important physiological signal, supported by and highly sensitive to the activity of voltage-gated Ca^{2+} channels. After membrane depolarization, Ca^{2+} channels first open but then undergo various forms of negative feedback regulation including voltage- and calcium-dependent inactivation (VDI and CDI, respectively). Inactivation of Ca^{2+} channel activity is perturbed in a rare yet devastating disorder known as Timothy syndrome (TS), whose features include autism or autism spectrum disorder along with severe cardiac arrhythmia and developmental abnormalities. Most cases of TS arise from a sporadic single nucleotide change that generates a mutation (G406R) in the pore-forming subunit of the L-type Ca^{2+} channel $Ca_V1.2$. We found that the TS mutation powerfully and selectively slows VDI while sparing or possibly speeding the kinetics of CDI. The deceleration of VDI was observed when the L-type channels were expressed with β_1 subunits prominent in brain, as well as β_2 subunits of importance for the heart. Dissociation of VDI and CDI was further substantiated by measurements of Ca^{2+} channel gating currents and by analysis of another channel mutation (I1624A) that hastens VDI, acting upstream of the step involving Gly^{406}. As highlighted by the TS mutation, CDI does not proceed to completeness but levels off at ≈50%, consistent with a change in gating modes and not an absorbing inactivation process. Thus, the TS mutation offers a unique perspective on mechanisms of inactivation as well as a promising starting point for exploring the underlying pathophysiology of autism.

autism | autism spectrum disorder | channelopathy | mutation | arrhythmia

Autism and autism spectrum disorders (ASD) are a continuum of debilitating and mysterious neurodevelopmental disorders, typified by impaired social interaction and communication skills and restricted and repetitive behavior. Despite great interest in ASD, their etiology remains largely unknown. However, genetic evidence supports the notion that the roots of the pathology will ultimately be uncovered at the level of cellular and developmental neurobiology and that insights into fundamental mechanisms may emerge from studies of rare forms of the disease with simple genetic origin. Accordingly, increasing attention has been directed toward Timothy syndrome (TS), a rare childhood disorder whose manifestations include a very strong association with autism or ASD ($P = 1.2 \times 10^{-8}$) along with abnormally prolonged cardiac action potentials and a wide-ranging set of developmental abnormalities. TS was identified in 1992 (1–3), but its likely importance as an exemplar only came into sharp focus a dozen years later, when Splawski *et al.* (4) showed that the diverse symptoms of TS could be traced in most cases to a single amino acid defect in a single protein molecule. The mutation (a Gly-to-Arg missense mutation at position 406) was identified in a well known signaling molecule, the pore-forming subunit of the class C ($Ca_V1.2$) L-type Ca^{2+} channel. Recently, a mouse model of TS bearing the Gly-to-Arg mutation was reported to exhibit behavioral characteristics reminiscent of ASD.[‡] That TS arises from a mutation in $Ca_V1.2$ is particularly instructive because this L-type Ca^{2+} channel is critically important for electrical activity, development, and effector signaling in major organs targeted by TS, including brain and heart.

What is the functional impact of the mutation at the cellular level? When introduced into rabbit recombinant $Ca_V1.2$ channels, the TS mutation produced no obvious changes in either the voltage dependence of channel activation or the level of channel expression (4). However, the mutation greatly impaired the ability of the channels to stop conducting during depolarization, a process known generically as inactivation. These results raised a series of questions about the basic mechanism by which the G406R mutation affects channel function. First, because inactivation of voltage-gated Ca^{2+} channels is strongly affected by the identity of the auxiliary β subunit, is the effect of the TS mutation on L-type channels equally prominent regardless of whether the β subunit is typical of those found in either heart or brain? Second, how strong are the effects of the TS mutation when studied in combination with other amino acid changes that themselves affect inactivation? Third, L-type channels display multiple forms of negative feedback, including voltage-dependent inactivation (VDI), which can be studied with Ba^{2+} or Na^+ as the charge carrier, and calcium-dependent inactivation (CDI), observed with Ca^{2+} as the permeant ion (5–7). Given proposals that VDI and CDI share the same final common pathway (8, 9), do G406R and other mutations affect both forms of inactivation in the same general way? Answers to these questions would help clarify mechanisms of inactivation and also provide useful clues for future explorations of the higher-order effects of the TS mutation in its primary organ targets, including the autistic brain.

Results

The TS Mutation Slows Inactivation of $Ca_V1.2$ Irrespective of the Coexpressed β Subunit. We began by examining the effect of the TS mutation in the context of various calcium channel accessory subunits. The β subunit subtype varies widely among tissues affected by TS and profoundly influences Ca^{2+} channel inactivation (8, 10). For example, β_2 (predominant in heart) confers much slower inactivation than β_1 (prominent in brain). Whereas Splawski *et al.* (4) studied β_{2b}, we chose β_{2a}, also found in heart,

Author contributions: C.F.B. and R.W.T. designed research; C.F.B. performed research; C.F.B. analyzed data; and C.F.B. and R.W.T. wrote the paper.

The authors declare no conflict of interest.

Freely available online through the PNAS open access option.

*Present address: Departments of Neurology and Human Genetics, Leiden University Medical Center, Leiden, The Netherlands.

†To whom correspondence should be addressed at: Stanford University School of Medicine, Beckman Center, Room B105, Stanford, CA 94305-5345. E-mail: rwtsien@stanford.edu.

This article contains supporting information online at www.pnas.org/cgi/content/full/0710501105/DC1.

‡Wersinger SR, Hesse RA, Badura MA, Bett GCL, Rasmussen RL, 2007 Society for Neuroscience Annual Meeting, November 3–7, 2000, San Diego, CA, abstr. 62.6.

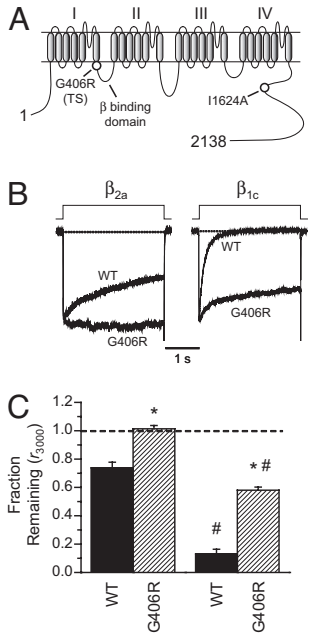

Fig. 1. The TS (G406R) mutation slows VDI irrespective of the coexpressed β subunit. (*A*) Secondary structure of the $Ca_V1.2$ α_{1C} subunit. The approximate locations of mutations G406R and I1624A are indicated. (*B*) Exemplar normalized Ba^{2+} currents recorded from WT and G406R channels expressed with either β_{2a} (*Left*) or β_{1c} (*Right*) together with $\alpha_2\delta$. Currents were elicited by step depolarization to +10 mV from a holding potential of −90 mV. (*C*) Summary of fraction remaining at 3 s. *, $P < 0.001$ versus WT; #, $P < 0.001$ versus β_{2a}.

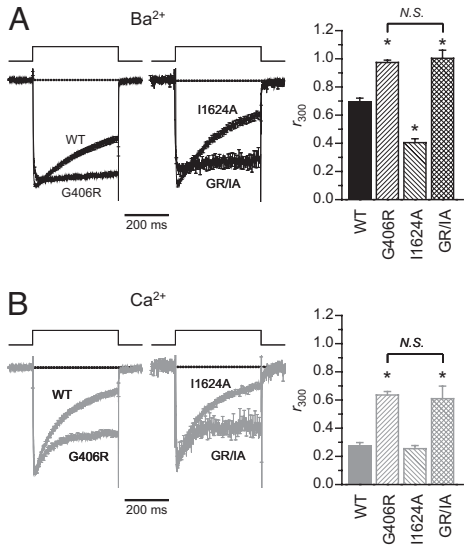

Fig. 2. G406R slows current decay for both WT and I1624A channels regardless of charge carrier. (*Left*) Normalized whole-cell currents elicited in Ba^{2+} (*A*) or Ca^{2+} (*B*). Step depolarizations (400-ms) were applied to +10 mV from a holding potential of −90 mV. Shown are average traces ± SEM. (*Right*) Summary of fraction remaining after 300 ms. *, $P < 0.001$ versus WT. Note that G406R and G406R/I1624A currents did not differ significantly (N.S.) with either charge carrier.

because it confers the slowest inactivation of all known β subunits and thus provides the most extreme case for probing the effect of the TS mutation. Slowed inactivation by β_{2a} is by virtue of a palmitoylation site (unique among the β subunits) that supports anchoring to the plasma membrane (11, 12). Accordingly, we tested whether the TS mutation might affect inactivation even in the context of the β_{2a} subunit. Whole-cell currents were recorded from $Ca_V1.2$ channels coexpressed with β_{2a} and $\alpha_2\delta$, using prolonged step depolarizations (Fig. 1*B*), with Ba^{2+} as the charge carrier to examine VDI; fractional current remaining at 3 s ($r_{3,000}$) was used as a metric of channel inactivation (13). Wild-type channels exhibited only modest inactivation after 3 s at 10 mV, as expected with the β_{2a} subunit (8). In the context of the β_{2a} subunit, the TS mutation powerfully slowed VDI; indeed, virtually all inactivation was abolished (Fig. 1 *B* and *C*). This incremental effect of the TS mutation is consistent with the cardiac manifestations of the disorder, which include a considerable prolongation of the ventricular action potential as reflected by the long Q–T interval of the electrocardiogram (14).

We turned next to testing the effect of the TS mutation in the context of the neuronal β_1 subunit. Given that G406R hampered VDI in a setting where inactivation was already weak (with β_{2a}), it was of interest to see whether the mutation was comparably effective when basal inactivation was relatively strong. A β_1 isotype was chosen as an exemplar of a β subunit common in the brain. Relative to β_{2a}, significantly more VDI was observed with the β_{1c} subunit, yet the TS mutation once again powerfully slowed VDI (Fig. 1 *B* and *C*). In fact, β_{1c} revealed the true power of the TS mutation in slowing inactivation: with β_{1c}, the mutation reduced VDI by ≈45% compared with only a ≈27% reduction with β_{2a}. The overall conclusion is that the TS mutation is able to influence the development of VDI regardless of whether the resident β subunit confers fast or slow VDI. In subsequent experiments, we examined inactivation in channels containing β_{1c}, thus providing ample dynamic range for mutations to have an effect.

Testing Effects of G406R in Combination with Another Mutation in α_{1C}. The C terminus of $Ca_V1.2$ contains an IQ motif (Ile^{1624}–Gln^{1625}) implicated in mediating CDI (15, 16). As shown using *Xenopus* oocytes (15, 17), mutating the Ile to an Ala (I1624A) significantly accelerated VDI (Fig. 2*A*). Given that Ile^{1624} is located in the C terminus of the channel, >1,000 residues away in primary sequence from the IS6 segment that harbors Gly^{406} (see Fig. 1*A*), we wondered whether the functional contributions of these structural elements would be exerted at the same or different stages in the signaling pathway leading up to inactivation. Accordingly, we asked whether mutating these critical amino acids in combination would lead to a summation of the effects of the individual mutations or instead would reveal a dominant influence of one over the other, reflecting an action further along the signaling pathway. When examined in the context of I1624A, the G406R mutation dominated, as the GR/IA double mutant channels exhibited VDI and CDI profiles that were indistinguishable from channels bearing G406R alone (Fig. 2), which suggests that the slowing effect of the TS mutation lies downstream of where I1624A acts to accelerate VDI. One possibility is that the IQ motif acts as a latch to brake the initiation of inactivation (17, 18), and even when the I1624A mutation releases the latch, VDI remains intrinsically slowed by the G406R mutation.

Is CDI Spared by Mutations that Slow or Accelerate VDI? A closer examination of the inactivation data (Figs. 2 and 3*A*) revealed that whether VDI is slowed by G406R or speeded by I1624A, Ca^{2+} still exerts a significant effect on whole-cell currents, increasing decay in the cases of both mutations. This finding led us to consider the possibility that CDI might proceed independently from VDI, developing with its own kinetics regardless of whether VDI is intact, slowed or accelerated. The approach taken to address this possibility (Fig. 3*A*, *Lower*) is based on experiments shown in Fig. 3*B*.

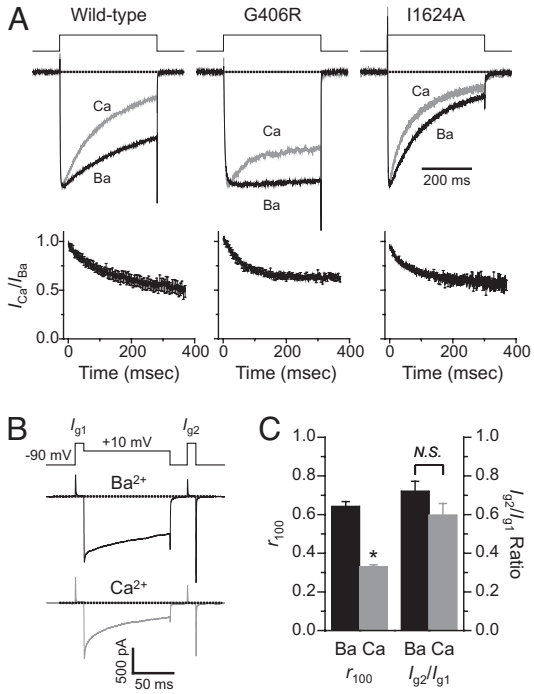

Fig. 3. CDI is spared by mutations that slow or accelerate VDI. (*A*) (*Upper*) Exemplar normalized Ba^{2+} and Ca^{2+} currents recorded at +10 mV from WT, G406R, and I1624A channels. (*Lower*) Ratio plots of normalized I_{Ca}/I_{Ba} currents. Shown are average plots ± SEM; the data were not significantly different as determined with either ANOVA or unpaired Student's *t* test. (*B*) Exemplar currents elicited using the voltage protocol indicated, with either Ba^{2+} or Ca^{2+} as the charge carrier. The pulses labeled I_{g1} and I_{g2} were to E_{rev} (see below). (*C*) Summary of inactivation and gating charge immobilization with either Ba^{2+} or Ca^{2+}. For every cell recorded, E_{rev} was determined empirically; with Ba^{2+} or Ca^{2+} as the charge carrier, E_{rev} was 59.4 ± 1.4 mV and 81.9 ± 2.0 mV, respectively. *, $P < 0.001$ versus Ba^{2+}. N.S., not significant.

VDI but Not CDI Causes Gating Charge Immobilization. To disentangle VDI and CDI and to test whether these processes may be partially or largely independent, we turned to measurements of gating charge movement. Conventional VDI of ion channels involves a transition into an absorptive state in which the gating charge becomes immobilized. A classic example of this mechanism is the ball-and-chain model of *Shaker* potassium channel inactivation, in which an N-terminal particle (the "ball") binds to the pore of the channel (19–23). A similar mechanism, only using the intracellular loop connecting the first and second domains of the channel (the I–II loop), has been proposed to mediate inactivation of L-type Ca^{2+} channels (8, 24, 25). If CDI of L-type Ca^{2+} channels were mediated by the same effector mechanism as VDI, we would expect both processes to cause gating charge immobilization. However, using a photolabile chelator, Hadley and Lederer (26; but see also 27) found that uncaging of intracellular Ca^{2+} caused CDI but not gating charge immobilization.

We reexamined the question of whether CDI causes charge immobilization by using an approach geared to CDI produced physiologically, by Ca^{2+} influx through the channel itself. To dissociate gating charge movement from ionic current, gating currents were isolated by a sudden depolarization to the reversal potential (E_{rev}), where ionic current is zero. This method was validated by bath application of the pore blocker La^{3+} (28–30). In the continued presence of 10 mM Ca^{2+}, 5.2 mM La^{3+} reduced the peak ionic current by >90% but was without effect on gating currents elicited at E_{rev} [supporting information (SI) Fig. 6].

To look for a possible effect of CDI on gating charge immobilization, we used a multipulse protocol (Fig. 3*B*). First, a gating current was elicited by stepping to E_{rev} for 10 ms (I_{g1}), after which the membrane was stepped to +10 mV for 100 ms to permit ion flux. After a 20-ms step back to −90 mV (of sufficient length to close the channels yet brief enough to allow only minimal recovery from inactivation), a second gating current was elicited at E_{rev} (I_{g2}). The ratio of the second gating current to the first (I_{g2}/I_{g1}) provided a measure of gating charge immobilization during the 100 ms at +10 mV. Currents were first recorded in Ba^{2+} to express VDI, then with the Ba^{2+} replaced by Ca^{2+} to drive CDI. As illustrated by representative current traces (Fig. 3*B*) and pooled data (Fig. 3*C*), the extent of the current decay was significantly greater with Ca^{2+} than with Ba^{2+}, consistent with CDI; the disparity in the fraction of peak current remaining after 100 ms (r_{100}) was ≈2-fold (Fig. 3*C*). Notably, however, the ratio of gating charge movements was not significantly affected by prior entry of Ca^{2+}. Thus, Ca^{2+} influx hastened the inactivation of ionic current, CDI, without affecting the immobilization of gating charge.

VDI and CDI Treated as Proceeding with Independent Probabilities. Our gating current measurements suggested that CDI might be mediated by an effector mechanism distinct from VDI. It was therefore appropriate, at least approximately, to treat them as separate processes, each with its own probability of allowing the channel to conduct ($P_{conduct}$). Moreover, the probability that the channel is not inactivated (and hence conducting) at any given time during the depolarization can be represented by the product of h_V and h_{Ca} (which are the probabilities that the channel has not undergone VDI or CDI, respectively). Thus, during the decaying phase of whole-cell Ca^{2+} current,

$$I_{Ca} \propto P_{conduct} \approx h_V \cdot h_{Ca}, \quad [1]$$

whereas with Ba^{2+} as the charge carrier, $h_{Ca} \approx 1$, and therefore,

$$I_{Ba} \propto P_{conduct} \approx h_V. \quad [2]$$

To a good approximation, h_{Ca} then can be determined by taking the ratio of I_{Ca} to I_{Ba}, measured within the same cell, thus providing a useful way to measure CDI in isolation. It is important to note that CDI is frequently expressed as the difference between VDI and CDI (16, 31–34). However, such an approach can potentially fail to account for changes in VDI. For example, when VDI is accelerated (e.g., by the I1624A mutation), simply subtracting CDI from VDI can underestimate the effects of Ca^{2+} on inactivation. To avoid this complication, we assessed CDI as the decrement in the running I_{Ca}/I_{Ba} ratio during the course of a 400-ms depolarization (Fig. 3*A*). Expressed in this way, the I_{Ca}/I_{Ba} ratio (h_{Ca}) of wild-type channels decays by ≈50% over the course of a 400-ms test depolarization. Using this metric, we found that the extent of CDI was similar in channels bearing either the G406R or I1624A mutation.

Importantly, the ratio for G406R channels decayed significantly faster than wild type (WT): when the I_{Ca}/I_{Ba} ratio plots were fitted with single exponentials, we found that the time constant averaged 55 ± 8 ms for G406R compared with 142 ± 18 ms for WT ($P < 0.005$). Thus, CDI was not only intact in G406R channels but proceeded more rapidly than in WT channels. CDI measured for I1624A channels decayed at a rate similar to WT channels (105 ± 14 ms; $P = 0.4$ vs. WT).

The G406R Mutation Reveals That CDI Cannot Be an Absorptive Form of Inactivation. The large extent to which the G406R mutation slowed VDI provided a fresh opportunity to study CDI with relatively little interference from VDI (that is, with $h_V \approx 1$). Our gating current measurements indicate that CDI is not associated with charge immobilization and thus might differ from VDI in other

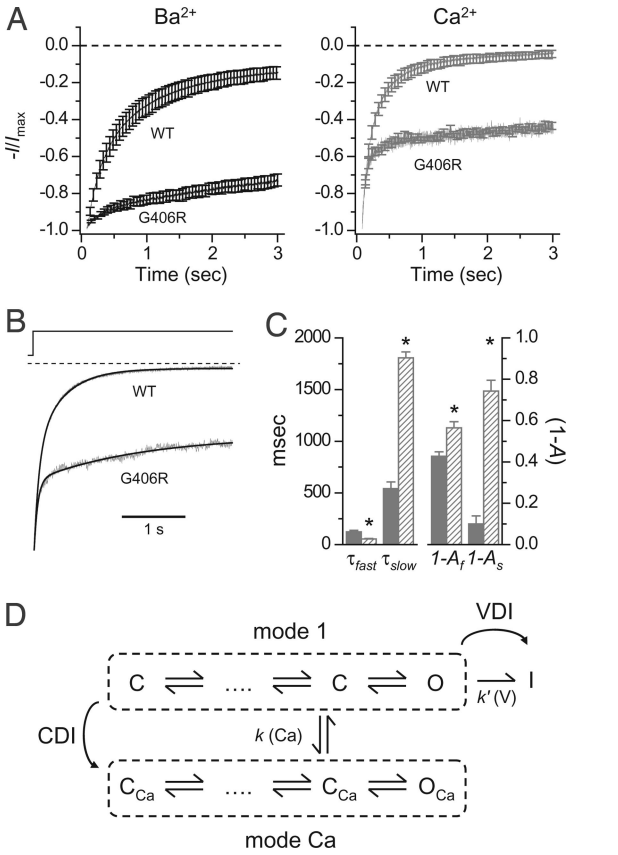

Fig. 4. The G406R mutation slows VDI and accelerates CDI. (*A*) Whole-cell Ba^{2+} or Ca^{2+} currents were elicited at +10 mV and normalized to the peak inward current. Shown are average currents ± SEM. (*B*) Normalized Ca^{2+} currents from two exemplar cells. The dashed line indicates zero current level, and the solid lines are fits to the product of two exponentials (see *Materials and Methods*). (*C*) Summary of the fitting parameters for WT (solid bars) and G406R (hatched) Ca^{2+} currents, as in *B*. *, $P < 0.01$ vs. WT. (*D*) Gating scheme showing transitions through the various proposed states. C, closed; O, open; I, inactivated. In Ba^{2+}, channels predominantly display mode 1 gating followed by transitioning to the inactivated state (VDI). With Ca^{2+} as the charge carrier, open channels rapidly transition to mode Ca (39, 40), displaying reduced P_o (CDI).

fundamental respects. To test whether CDI is an absorbing event, proceeding unidirectionally at inactivating membrane voltages, we again turned to prolonged (3-s) depolarizations and measured currents by using either Ba^{2+} or Ca^{2+} as the charge carrier. As already shown in Fig. 1, the TS mutation dramatically slowed inactivation in Ba^{2+} (Fig. 4*A*, *Left*). Interestingly, when Ca^{2+} was the charge carrier, G406R currents exhibited a rapid decay to ≈50% amplitude, and this decay was followed by a very slowly decaying plateau (Fig. 4*A*, *Right*). Based on the gating current-based logic as described earlier, we analyzed the overall current decay as the product of two terms, one for CDI and the other for VDI (see *Materials and Methods*). For simplicity, each of the factors was described as a partially decaying exponential, as in the classical description of sodium channel inactivation (35).

The decaying phase of the Ca^{2+} currents in Fig. 4*A* were well described by such an equation, as illustrated by exemplar fits (Fig. 4*B*); the fitting parameters are summarized in Fig. 4*C*. The TS mutation greatly slowed the slow time constant (τ_{slow}), as expected for slowed VDI, whereas the fast time constant (τ_{fast}) was not slowed at all, but in fact became >2-fold faster (124 ± 14 ms vs. 54 ± 4.7 ms). When analyzed in this way, the extent of CDI was generally unaffected by the TS mutation. The fraction of G406R channels remaining noninactivated after CDI ($h_{Ca,\infty} = 1 - A_{fast}$) was ≈50%, which underscores the idea that CDI cannot be regarded as an absorptive process, proceeding toward a steady-state value of zero, but reflects instead a reversible balance between two conditions of different open probability (Fig. 4*D*, and see *Discussion*).

Discussion

The TS mutation G406R is an exemplar of a disease-causing missense mutation (channelopathy) that not only provides insight into the workings of a key signaling molecule but also offers a toehold in understanding a complex human disorder (36). This recurrent *de novo* mutation in $Ca_V1.2$ L-type Ca^{2+} channels produces an unusually wide range of phenotypic effects on multiple organs (4). In two of these systems, heart and brain, excitable cells rely on L-type Ca^{2+} channels for important aspects of development and physiology (37, 38). Our experiments focused on altered properties of L-type channel currents and also support a bottom-up approach to higher-order dysfunction, including arrhythmia and autism, that arise from the single gene defect.

Building on the work of Splawski *et al.* (4), who described effects of G406R on VDI, we used G406R and other structural modifications to probe the basis of VDI and CDI. How does the TS mutation match up with other structural modifications that affect inactivation of L-type channels? Do VDI and CDI share a common final step, as often suggested? We approached these questions by recording both Ba^{2+} and Ca^{2+} currents in the same cells, under patch-clamp recording conditions where ionic and gating currents could be isolated and VDI and CDI could be appropriately dissected. We found that G406R exerted powerful effects on inactivation of expressed $Ca_V1.2$ channels: the TS mutation greatly slowed VDI while speeding the kinetics of CDI. This slowing of VDI was observed irrespective of whether the auxiliary β subunit was typical of heart or brain. Furthermore, VDI caused immobilization of gating charge, whereas CDI did not, even when evoked in a physiological manner, by Ca^{2+} entry through the L-type channel itself. Our data support the idea that CDI does not reflect an absorptive transition to an inactivated state but arises instead from a Ca^{2+}-dependent transition to a gating mode with decreased P_o, for example, by switching from mode 1 to mode calcium gating (39), or from mode 2 to mode 1 gating (40).

Our results provide a fresh perspective on earlier studies of L-type channel inactivation approached with other structural interventions. VDI is slowed in chimeric L-type Ca^{2+} channels in which the I–II loop of host $Ca_V1.2$ subunits is replaced by the corresponding region of $Ca_V1.1$ channels that lack CDI (41). In contrast, CDI (at least as we have defined it here) was hardly affected in those chimeric channels, suggesting that the region mediating VDI (the I–II loop) may not play a role in mediating CDI. Likewise, the recordings of Cens *et al.* (8) for $Ca_v1.2$ expressed with different β subunits showed a dramatic effect of β subunit identity on the time course of inactivation with Ca^{2+} as the charge carrier. However, if one allows for the idea that VDI can proceed unchecked even while Ca^{2+} permeation takes place, the extra degree of inactivation that is specifically Ca^{2+}-dependent (CDI) appears unchanged in their data.[§] Thus, we contend that both switching of β subunits and swapping of the I–II loop (a region of known importance for β subunit interactions) provide support for a dissociation between VDI and CDI, consistent with the effects of G406R presented here. Taken together, all of these structurally based interventions reinforce

[§]The authors arrived at a different conclusion because they used "CDI" to denote inactivation (decay of whole-cell current amplitude) in the presence of Ca^{2+} rather than the extra decay that is specifically Ca^{2+}-dependent.

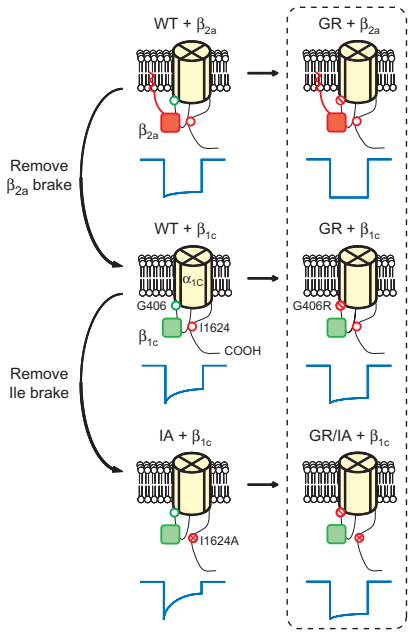

Fig. 5. Proposed model to account for our findings with VDI. For simplicity, only the α_1 and β subunits of the channel are shown, and only the I–II loop and C-terminal tail of the α_1 subunit are depicted; other regions have also been reported to contribute to VDI (52–54). Approximate positions of Gly^{406} and Ile^{1624} are shown by green and red circles, respectively. Shown below are idealized whole-cell Ba^{2+} currents. VDI of $Ca_V1.2$ L-type calcium channels is mediated by the concerted actions of several converging intrinsic and extrinsic interactions. (*Top*) WT channels expressed with the cardiac β_{2a} subunit exhibit slowed VDI because of the presence of a unique palmitoylation moiety on β_{2a}. (*Middle*) Replacing β_{2a} with the brain β_1 subunit speeds up VDI. (*Bottom*) The IQ motif appears to serve as a Ca^{2+}-independent brake against VDI, possibly by association with the hinged lid of the I–II loop. The I1624A mutation may disrupt this interaction, thereby accelerating VDI. Under all conditions, the effect of the TS mutation (G406R, dashed box) is to slow VDI powerfully.

the earlier notion that VDI and CDI are mediated by distinct effector mechanisms (5, 26).

Further analysis was performed on the effects of a previously described mutation, I1624A, in a region of the $Ca_V1.2$ α_1 subunit, the C-terminal IQ motif, where partial structural information is available. Like the TS mutation, I1624A altered VDI, but in this case by acceleration rather than slowing. Once again, CDI was dissected as a multiplicative factor and was found to be essentially spared. For purposes of epistasis analysis, the effects of I1624A were also studied in combination with G406R. Our results indicate that the influence on VDI by I $\rightarrow$ A occurs at least one step upstream to that affected by G $\rightarrow$ R. Our findings on the effects of β subunit switching, I1624A and G406R, on VDI are summarized in diagram form in Fig. 5 (see legend for details).

Our data in HEK293 cells revealed several key differences from previous findings in *Xenopus* oocytes (15, 17), although the same constructs for WT and mutant $Ca_V1.2$ channels were used. In the oocyte recordings, I1624A Ca^{2+} or Ba^{2+} currents decayed with a similar time course, and thus the channels appeared to lack CDI altogether. In contrast, when expressed in human embryonic kidney (HEK) cells, we found that I1624A channels exhibit essentially normal CDI (Fig. 3). One possible explanation for this discrepancy is that in oocytes, CDI was obscured by a robust Ca^{2+}-dependent facilitation (CDF) that occurred even during a single depolarizing pulse,[¶] which may have been less problematic in the mammalian cells studied here; I1624A channels showed considerably less CDF in HEK cells than in oocytes when evoked by pulse trains (data not shown).

Our findings with I1624A mutant channels help provide insight into the role of the IQ motif in mediating VDI and CDI. Consistent with previous results (15, 17), we found that the I1624A mutation accelerates VDI. However, unlike previous results and as described above, in our hands this accelerated VDI fails to occlude CDI, consistent with biochemical (17) and structural (42, 43) data, suggesting that the interaction of the channel with calmodulin, a Ca^{2+}-dependent associated protein required for CDI (15), is unaffected by the mutation.

In summary, our evidence supports the notion that VDI and CDI occur with independent probabilities, likely through independent mechanisms. We propose that a shift to low-P_o gating, and not an absorptive inactivated state, underlies CDI. This alternate way of interpreting CDI can be helpful in trying to understand channelopathies that affect inactivation of Ca^{2+} channels. Such mutations include congenital stationary night blindness type 2 in $Ca_V1.4$ (44) as well as TS in $Ca_V1.2$ (4, 45).

Splawski *et al.* (4) presented compelling evidence for how the classical TS mutation, and an additional mutation that can generate a related disorder known as TS2 (45), can lead to prolonged cardiac action potentials, excessive Ca^{2+} entry, and arrhythmias involving Ca^{2+} overload. This scenario is supported by the finding that the L-type Ca^{2+} channel antagonist verapamil decreased ventricular arrhythmia in a patient with TS (46) and a recent report that the L-type agonist Bay K 8644 recapitulates many of the cardiac features of TS (47). Compared with arrhythmias, understanding autism from the ground up will likely be even more challenging. The use of agents like Bay K 8644 may serve as pharmacological mimics of the TS mutation by promoting an increase in L-type Ca^{2+} entry and possibly a shift in gating mode as well (48), a possibility not excluded by our findings on VDI. It would be interesting to test the effects of such pharmacological interventions on brain circuits of possible significance to ASD.

Materials and Methods

Generation of α_{1C} Constructs. The human α_{1C} ($Ca_V1.2$) splice variant 77 (pHLCC77; GenBank accession no. CAA84346) (49–51) used in this work was a kind gift from Roger Zühlke and Harald Reuter (University of Bern, Bern, Switerland). The cDNA of WT and I1624A human $\alpha_{1C,77}$ (15) was subcloned into pcDNA3.1 for expression in mammalian cells. The TS mutation G406R was introduced by mutating the codon GGA to AGA by using the QuikChange II XL site-directed mutagenesis kit (Stratagene); sequencing verified the mutation and the fidelity of the remaining construct. The I1624A/G406R double mutant was generated by subcloning the C terminus of the I1624A cDNA into the G406R construct.

Cell Culture. HEK293 cells stably expressing the calcium channel auxiliary β_{1c} and $\alpha_2\delta$-1 subunits were cultured and transfected as described in ref. 30 by using either Lipofectamine 2000 (Invitrogen) or calcium phosphate precipitation (Clontech). Cells were transfected with either WT or mutant $\alpha_{1C,77}$ constructs together with pEGFP-N3, and currents were recorded 24–48 h after transfection. For the data in Fig. 1, tsA201 cells were transfected with WT or mutant $\alpha_{1C,77}$ together with pEGFP-N3 and the calcium channel subunits $\alpha_2\delta$-1 and either β_{2a} or β_{1c} (kind gifts from Gerald Zamponi, University of Calgary, Calgary, BC, Canada) and recorded 24–48 h after transfection. The data in Fig. 3 *B* and *C* were generated from a stable HEK293 cell line expressing WT $\alpha_{1C,77}$ with an IRES-EGFP, β_{1c} and $\alpha_2\delta$-1.

Electrophysiology. Whole-cell currents were recorded at room temperature by using an Axopatch 200B patch-clamp amplifier (Molecular Devices). Borosilicate glass capillaries were pulled in a model P-87 or P-97 puller (Sutter Instruments) and heat-polished before use. Pipette resistance was ≈2–3 MΩ when filled with an internal solution consisting of 122 mM Cs-Asp, 10 mM

[¶]Although CDF is most often seen as a progressive increase in Ca^{2+} currents during trains of depolarizing pulses or after a conditioning pulse, it can also occur during a single pulse. This was most obvious in $Ca_V1.2$ subunits bearing the IQ/AA double mutation, where CDF is most strongly apparent (17): IQ/AA channels exhibited "negative" CDI (that is, less decay in Ca^{2+} than in Ba^{2+}), consistent with the principle that CDF can obscure CDI.

Hepes, 10 mM EGTA, 5 mM $MgCl_2$, 4 mM ATP, 0.4 mM GTP, pH 7.5. The bath solution contained 155 mM NMDG-Asp, 0.1 mM EGTA, 10 mM Hepes, 10 mM $BaCl_2$ or $CaCl_2$, pH 7.4. Series resistance (8.95 ± 1.1 MΩ) was compensated electronically by ≥90%, and membrane capacitance (19.6 ± 0.9 pF) was corrected online; where applicable, residual linear capacitive and leak currents were subtracted by the $-P/4$ method.

EGFP-positive cells were visualized by epifluorescence and selected for recording. Cells were voltage-clamped at −90 mV, and pulse depolarizations were applied at 10-s intervals. Data were passed through a four-pole low-pass Bessel filter at 1–10 kHz, digitized at 5–100 kHz with a Digidata 1320A (Molecular Devices), and stored on a personal computer.

Data Analysis. Data were acquired and analyzed with pClamp 8.2 (Molecular Devices). Summary data are presented as mean ± SEM, and $n = 4$–12 cells per condition. Statistical significance was tested by using a two-tailed Student's unpaired t test, except where indicated.

The fits in Fig. 4 were calculated by using the equation:

$$I = [(1 - A_{\text{fast}}) + A_{\text{fast}} e^{-t/\tau_{\text{fast}}}] \, [(1 - A_{\text{slow}}) + A_{\text{slow}} e^{-t/\tau_{\text{slow}}}] \quad [3]$$

where I is normalized current amplitude, t is time in ms, A_{fast} and A_{slow} are the fast and slow amplitudes, respectively, and τ_{fast} and τ_{slow} are the fast and slow time constants, respectively.

ACKNOWLEDGEMENTS. We thank Roger Zühlke and Harald Reuter for providing the wild-type and I1624A cDNAs, Gerald Zamponi for providing accessory subunit cDNAs, and Harald Reuter and Damian Wheeler for helpful discussions. This work was supported by National Heart, Lung, and Blood Institute/National Institutes of Health Stanford Vascular Biology and Medicine Training Grant 5T32HL007708-14 (to C.F.B.) and National Institutes of Health Grants 5R01NS024067-22 and 5R01GM058234-08 (to R.W.T.).

1. Reichenbach H, Meister EM, Theile H (1992) *Kinderarztl Prax* 60:54–56.
2. Marks ML, Trippel DL, Keating MT (1995) *Am J Cardiol* 76:744–745.
3. Marks ML, Whisler SL, Clericuzio C, Keating M (1995) *J Am Coll Cardiol* 25:59–64.
4. Splawski I, Timothy KW, Sharpe LM, Decher N, Kumar P, Bloise R, Napolitano C, Schwartz PJ, Joseph RM, Condouris K, *et al*. (2004) *Cell* 119:19–31.
5. Lee KS, Marban E, Tsien RW (1985) *J Physiol* (*London*) 364:395–411.
6. Cens T, Rousset M, Leyris JP, Fesquet P, Charnet P (2006) *Prog Biophys Mol Biol* 90:104–117.
7. Budde T, Meuth S, Pape HC (2002) *Nat Rev Neurosci* 3:873–883.
8. Cens T, Restituito S, Galas S, Charnet P (1999) *J Biol Chem* 274:5483–5490.
9. Findlay I (2004) *J Physiol* (*London*) 554:275–283.
10. Sather WA, Tanabe T, Zhang JF, Mori Y, Adams ME, Tsien RW (1993) *Neuron* 11:291–303.
11. Chien AJ, Zhao X, Shirokov RE, Puri TS, Chang CF, Sun D, Rios E, Hosey MM (1995) *J Biol Chem* 270:30036–30044.
12. Chien AJ, Carr KM, Shirokov RE, Rios E, Hosey MM (1996) *J Biol Chem* 271:26465–26468.
13. Barrett CF, Rittenhouse AR (2000) *J Gen Physiol* 115:277–286.
14. Rosen MR (2002) *Circulation* 106:2173–2179.
15. Zühlke RD, Pitt GS, Deisseroth K, Tsien RW, Reuter H (1999) *Nature* 399:159–162.
16. Peterson BZ, DeMaria CD, Adelman JP, Yue DT (1999) *Neuron* 22:549–558.
17. Zühlke RD, Pitt GS, Tsien RW, Reuter H (2000) *J Biol Chem* 275:21121–21129.
18. Kim J, Ghosh S, Nunziato DA, Pitt GS (2004) *Neuron* 41:745–754.
19. Armstrong CM, Bezanilla F (1977) *J Gen Physiol* 70:567–590.
20. Zhou M, Morais-Cabral JH, Mann S, MacKinnon R (2001) *Nature* 411:657–661.
21. Bezanilla F, Perozo E, Papazian DM, Stefani E (1991) *Science* 254:679–683.
22. Hoshi T, Zagotta WN, Aldrich RW (1990) *Science* 250:533–538.
23. Zagotta WN, Hoshi T, Aldrich RW (1990) *Science* 250:568–571.
24. Bernatchez G, Talwar D, Parent L (1998) *Biophys J* 75:1727–1739.
25. Stotz SC, Hamid J, Spaetgens RL, Jarvis SE, Zamponi GW (2000) *J Biol Chem* 275:24575–24582.
26. Hadley RW, Lederer WJ (1991) *J Physiol* (*London*) 444:257–268.
27. Isaev D, Solt K, Gurtovaya O, Reeves JP, Shirokov R (2004) *J Gen Physiol* 123:555–571.
28. Bean BP, Rios E (1989) *J Gen Physiol* 94:65–93.
29. Jones LP, DeMaria CD, Yue DT (1999) *Biophys J* 76:2530–2552.
30. Barrett CF, Cao YQ, Tsien RW (2005) *J Biol Chem* 280:24064–24071.
31. Peterson BZ, Lee JS, Mulle JG, Wang Y, de Leon M, Yue DT (2000) *Biophys J* 78:1906–1920.
32. Zühlke RD, Reuter H (1998) *Proc Natl Acad Sci USA* 95:3287–3294.
33. Liang H, DeMaria CD, Erickson MG, Mori MX, Alseikhan BA, Yue DT (2003) *Neuron* 39:951–960.
34. Mori MX, Erickson MG, Yue DT (2004) *Science* 304:432–435.
35. Hodgkin AL, Huxley AF (1952) *J Physiol* (*London*) 116:497–506.
36. Ptacek LJ (1997) *Neuromusc Disord* 7:250–255.
37. Catterall WA (2000) *Annu Rev Cell Dev Biol* 16:521–555.
38. Piedras-Rentería ES, Barrett CF, Cao YQ, Tsien RW (2007) in *Calcium*: *A Matter of Life or Death*, eds Krebs J, Michalak M (Elsevier, New York), pp 127–166.
39. Imredy JP, Yue DT (1994) *Neuron* 12:1301–1318.
40. Erxleben C, Gomez-Alegria C, Darden T, Mori Y, Birnbaumer L, Armstrong DL (2003) *Proc Natl Acad Sci USA* 100:2929–2934.
41. Adams B, Tanabe T (1997) *J Gen Physiol* 110:379–389.
42. Fallon JL, Halling DB, Hamilton SL, Quiocho FA (2005) *Structure (London)* 13:1881–1886.
43. Van Petegem F, Chatelain FC, Minor DL, Jr (2005) *Nat Struct Mol Biol* 12:1108–1115.
44. Singh A, Hamedinger D, Hoda JC, Gebhart M, Koschak A, Romanin C, Striessnig J (2006) *Nat Neurosci* 9:1108–1116.
45. Splawski I, Timothy KW, Decher N, Kumar P, Sachse FB, Beggs AH, Sanguinetti MC, Keating MT (2005) *Proc Natl Acad Sci USA* 102:8089–8098.
46. Jacobs A, Knight BP, McDonald KT, Burke MC (2006) *Heart Rhythm* 3:967–970.
47. Sicouri S, Timothy KW, Zygmunt AC, Glass A, Goodrow RJ, Belardinelli L, Antzelevitch C (2007) *Heart Rhythm* 4:638–647.
48. Erxleben C, Liao Y, Gentile S, Chin D, Gomez-Alegria C, Mori Y, Birnbaumer L, Armstrong DL (2006) *Proc Natl Acad Sci USA* 103:3932–3937.
49. Soldatov NM, Bouron A, Reuter H (1995) *J Biol Chem* 270:10540–10543.
50. Zühlke RD, Bouron A, Soldatov NM, Reuter H (1998) *FEBS Lett* 427:220–224.
51. Soldatov NM (1992) *Proc Natl Acad Sci USA* 89:4628–4632.
52. Livneh A, Cohen R, Atlas D (2006) *Neuroscience* 139:1275–1287.
53. Bernatchez G, Berrou L, Benakezouh Z, Ducay J, Parent L (2001) *Biochim Biophys Acta* 1514:217–229.
54. Raybaud A, Dodier Y, Bissonnette P, Simoes M, Bichet DG, Sauve R, Parent L (2006) *J Biol Chem* 281:39424–39436.